J. Chem. Thermodynamics 40 (2008) 1064–1076

Contents lists available at ScienceDirect

J. Chem. Thermodynamics

journal homepage: www.elsevier.com/locate/jct

The equilibrium phase diagram of the magnesium–copper–yttrium system

Mohammad Mezbahul-Islam, Dmytro Kevorkov, Mamoun Medraj *

Department of Mechanical Engineering, Concordia University, 1455 de Maisonneuve Boulevard West, Montreal, Canada H3G 1M8

ARTICLE INFO

Article history:
Received 8 November 2007
Received in revised form 5 March 2008
Accepted 5 March 2008
Available online 15 March 2008

Keywords:
Ternary phase diagram
Thermodynamic modelling
Modified quasichemical model
Mg alloys

ABSTRACT

Thermodynamic modelling of the Mg–Cu–Y system is carried out as a part of thermodynamic database construction for Mg alloys. This system is being modelled for the first time using the modified quasichemical model which considers the presence of short range ordering in the liquid. A self-consistent thermodynamic database for the Mg–Cu–Y system was constructed by combining the thermodynamic descriptions of the constituent binaries, Mg–Cu, Cu–Y, and Mg–Y. All the three binaries have been re-optimized based on the experimental phase equilibrium and thermodynamic data available in the literature. The constructed database is used to calculate and predict thermodynamic properties, the binary phase diagrams and *liquidus* projections of the ternary Mg–Cu–Y system. The current calculation results are in good agreement with the experimental data reported in the literature.

1. Introduction

Magnesium alloys are getting considerable attention for automobile and aerospace applications because they are the lightest among the commercially available structural alloys. They have high specific properties but low corrosion resistance which limited their use. While metallic glass, a new class of wonder material, is attracting attention due to its high mechanical strength and good corrosion resistance [1]. Mg–Cu–Y alloy system is a promising candidate for metallic glass since it has the largest super cooled liquid region among other Mg-alloy systems [2–5].

Despite its importance, this system has not yet been modelled thermodynamically. Also, the available descriptions for the binaries are contradictory to each other and none of the assessment was done considering the presence of short range ordering in the liquid. Hence the main objective of this work is to construct a reliable thermodynamic database of the Mg–Cu–Y system using sound thermodynamic models. The three constituent binary systems Mg–Cu, Cu–Y, and Mg–Y were re-optimized using the modified quasichemical model for the liquid phase. This model has the ability to take into consideration the presence of short range ordering in the liquid.

2. Analytical descriptions of the thermodynamic models employed

The Gibbs free energy function used for the pure elements (Mg, Cu, and Y) are taken from the SGTE (Scientific Group Thermodata Europe) compilation of Dinsdale [6].

The Gibbs free energy of a binary stoichiometric phase is given by

$$G^{\phi} = x_i{}^0G_i^{\phi_1} + x_j{}^0G_j^{\phi_2} + \Delta G_f, \quad (1)$$

where ϕ denotes the phase of interest, x_i and x_j are mole fractions of elements i and j which are given by the stoichiometry of the compound, and are the respective reference states of elements i and j in their standard state and $\Delta G_f = a + b(T/\mathrm{K})$ represents the Gibbs free energy of formation of the stoichiometric compound. The parameters a and b were obtained by optimization using experimental data.

The Gibbs free energy of the terminal solid solutions is described by the following equation:

$$G^{\phi} = x_i{}^0G_i^{\phi} + x_i{}^0G_j^{\phi} + R(T/\mathrm{K})[x_i \ln x_i + x_j \ln x_j] + {}^{ex}G^{\phi}. \quad (2)$$

The excess Gibbs free energy ${}^{ex}G^{\phi}$ is described by the Redlich–Kister polynomial model [7].

The modified quasichemical model [8–10] was chosen to describe the liquid phases of the three constituent binaries. From the literature survey, it was found that all the three binary systems have a very high negative enthalpy of mixing. Also, the calculated entropy of mixing curves of the Cu–Y and Mg–Y systems assume m-shaped characteristics. All these are indications of the presence of short range ordering [8]. The modified quasichemical model has

* Corresponding author. Tel.: +1 514 848 2424x3146; fax: +1 514 848 3175.
E-mail address: mmedraj@encs.concordia.ca (M. Medraj).
URL: http://www.me.concordia.ca/~mmedraj (M. Medraj).

0021-9614/$ - see front matter © 2008 Elsevier Ltd. All rights reserved.
doi:10.1016/j.jct.2008.03.004

three distinct characteristics [8–10]: (i) it permits the composition of maximum short range ordering in a binary system to be freely chosen, (ii) it expresses the energy of pair formation as a function of composition which can be expanded as a polynomial in the pair fraction and the coordination numbers are permitted to vary with the composition, and (iii) the model can be extended to multi-component systems. The model has been discussed extensively in the literature [8–10] and will be outlined briefly here. The energy of pair formation can be expressed by the following equation:

$$\Delta g_{AB} = \Delta g^{\circ}_{AB} + \sum_{i\geqslant 1} g^{i\circ}_{AB} X^{i}_{AA} + \sum_{j\geqslant 1} g^{\circ j}_{AB} X^{j}_{BB}, \tag{3}$$

where Δg°_{AB}, $\Delta g^{i\circ}_{AB}$, and $\Delta g^{\circ j}_{AB}$ are the parameters of the model and can be expressed as functions of temperature ($\Delta g^{\circ}_{AB} = a + b(T/\mathrm{K})$). Also, the atom to atom coordination numbers, Z_A and Z_B, can be expressed as a function of composition and can be represented by the following equations:

$$\frac{1}{Z_A} = \frac{1}{Z^{A}_{AA}}\left(\frac{2n_{AA}}{2n_{AA}+n_{AB}}\right) + \frac{1}{Z^{A}_{AB}}\left(\frac{n_{AB}}{2n_{AA}+n_{AB}}\right), \tag{4}$$

$$\frac{1}{Z_B} = \frac{1}{Z^{B}_{BB}}\left(\frac{2n_{BB}}{2n_{BB}+n_{AB}}\right) + \frac{1}{Z^{B}_{BA}}\left(\frac{n_{AB}}{2n_{BB}+n_{AB}}\right), \tag{5}$$

where n_{ij} is the number of moles of (i–j) pairs, Z^{A}_{AA} and Z^{A}_{AB} are the coordination numbers when all nearest neighbours of an A atom are A or B atoms, respectively. The composition at maximum short range ordering is determined by the ratio Z^{B}_{BA}/Z^{A}_{AB}. Values of Z^{A}_{AB} and Z^{B}_{BA} are unique to the A – B binary system and should be carefully determined to fit the thermodynamic experimental data (enthalpy of mixing, activity, *etc.*). The value of Z^{A}_{AA} is common for all systems containing A as a component. In this work, the value of Z^{Mg}_{MgMg}, Z^{Cu}_{CuCu} and Z^{Y}_{YY} was chosen to be 6 because it gave the best possible fit for many binary systems and is recommended by Dr. Pelton's group [8–10]. The values of Z^{Mg}_{MgCu}, Z^{Y}_{CuMg}, Z^{Mg}_{MgY}, Z^{Y}_{YMg}, Z^{Y}_{CuY}, and Z^{Y}_{YCu} are chosen to permit the composition at maximum short range ordering in the binary system to be consistent with the composition that corresponds to the minimum enthalpy of mixing. These values are given in table 1. The tendency to maximum short range ordering near the composition 40 atomic per cent (at.%) Mg in the Mg–Cu system was obtained by setting $Z^{Mg}_{MgCu} = 4$ and $Z^{Y}_{CuMg} = 2$. For the Cu–Y system, maximum short range ordering near 30 at.% Y was obtained by setting $Z^{Y}_{CuY} = 3$ and $Z^{Y}_{YCu} = 6$. Similarly for the Mg–Y system, the tendency to maximum short range ordering near the composition 30 at.% Y was obtained by setting $Z^{Mg}_{MgY} = 2$ and $Z^{Y}_{YMg} = 4$.

The Gibbs free energy of intermediate solid solutions is described by the compound energy formalism as shown in the following equations:

$$G = G^{ref} + G^{ideal} + G^{excess}, \tag{6}$$

$$G^{ref} = \sum y^{l}_{i} y^{m}_{j} \ldots y^{q}_{k} {}^{0}G_{(i:j:\ldots:k)}, \tag{7}$$

$$G^{ideal} = R(T/\mathrm{K}) \sum_{l} f_l \sum_{i} y^{l}_{i} \ln y^{l}_{i}, \tag{8}$$

$$G^{excess} = \sum y^{l}_{i} y^{l}_{j} y^{m}_{k} \sum_{\gamma=0} {}^{\gamma}L_{(i,j):k} \times (y^{l}_{i} - y^{l}_{j})^{\gamma}, \tag{9}$$

where $i,j,\ldots k$ represent components or vacancy, l, m and q represent sub-lattices, y^{l}_{i} is the site fraction of component i on sub-lattice l, f_l is the fraction of sub-lattice l relative to the total lattice sites, ${}^{0}G_{(i:j:\ldots k)}$ represents a real or a hypothetical compound (end member) energy, and ${}^{\gamma}L_{(i,j)}$ represent the interaction parameters which describe the interaction within the sub-lattice.

Modelling of the intermetallic solid solution phases requires information regarding the crystal structure of the phases and their homogeneity range. From the crystallographic data summarized in table 2, the following model is applied to represent the $MgCu_2$ phase:

$$(\mathrm{Mg}\%, \mathrm{Cu})_8 : (\mathrm{Cu}\%, \mathrm{Mg})_{16}.$$

Here, the '%' denotes the major constituent of the sub-lattice. This model covers the $0 \leqslant X_{Mg} \leqslant 1$ composition range and, of course, includes the homogeneity range of $0.31 \leqslant X_{Mg} \leqslant 0.353$ which was reported by Bagnoud and Feschotte [11].

The crystal structure data of the Cu_6Y intermediate solid solution was obtained by Buschow and Goot [12] and are listed in table 3.

According to Buschow and Goot [12] some of the Yttrium atomic sites are occupied by a pair of Cu atoms, which can be described by the following model with two sub-lattices:

$$(\mathrm{Y}\%, \mathrm{Cu}_2)(\mathrm{Cu})_5$$

This is actually a Wagner–Schottky type model [13]. The same model was used by Fries *et al.* [14] to represent Cu_6Y in their assessment of the Cu–Y system. This type of model can be used only for intermediate phases with a narrow homogeneity range [15]. This model covers $0.83 \leqslant X_{Cu} \leqslant 1$ composition range. This range includes homogeneity $0.84 \leqslant X_{Cu} \leqslant 0.87$ which was reported by Fries *et al.* [14]. The optimized model parameters are listed in table 4.

TABLE 1
Atom–atom "coordination numbers" of the liquid

A	B	Z^{A}_{AB}	Z^{B}_{AB}
Mg	Mg	6	6
Cu	Cu	6	6
Y	Y	6	6
Mg	Cu	4	2
Cu	Y	3	6
Mg	Y	2	4

3. Experimental data evaluation

According to the CALPHAD method, the first step of the thermodynamic optimization is to extract and categorize the available

TABLE 2
Crystal structure and lattice parameters of $MgCu_2$ phase

Phase	Crystal data		Atom	WP[a]	CN[b]	Atomic position			Reference
						X	*Y*	*Z*	
$MgCu_2$	Prototype	$MgCu_2$	Cu	16d	12	0.625	0.625	0.625	[68]
	Pearson symbol	cF24	Mg	8a	16	0	0	0	
	Space group	$Fd\bar{3}m$							
	Space group No.	227							
	Lattice parameter/nm	$a = 0.7035$							[11]
	Angles: $\alpha = 90°$, $\beta = 90°$, $\gamma = 90°$								

[a] WP, Wyckoff Position.
[b] CN, coordination number.

TABLE 3
Crystal structure and lattice parameters of Cu_6Y phase

Phase	Crystal data		Atoms	WP[a]	CN[b]	Atomic position			References
						X	Y	Z	
Cu_6Y	Prototype	$TbCu_7$	Y	1a	20	0	0	0	[12]
	Pearson symbol	*hP8*	Cu 1	2e	8	0	0	0.306	
	Space group	*P6/mmm*	Cu 2	2c	12	0.333	0.667	0	
	Space group No.	191	Cu 3	3g	16	0.5	0	0.5	
	Lattice parameter/nm	$a = 0.4940$							
		$b = 0.4157$							
	Angles: $\alpha = 90°$, $\beta = 90°$, $\gamma = 120°$								

[a] WP, Wyckoff position.
[b] CN, coordination number.

TABLE 4
Optimized model parameters for the liquid, Mg-hcp, Cu-fcc, Mg_2Cu and $MgCu_2$phases in the Mg–Cu system

Phase	Terms	$a/(J \cdot mol^{-1})$	$b/(J \cdot mol^{-1} \cdot K^{-1})$
Liquid	Δg°_{AB}	−12975.95	0
	g°_{AB}	−6153.13	1.26
	$g^{\circ j}_{AB}$	−13528.50	0
Mg-hcp	${}^0L^{Mg\text{-}hcp}$	8371.60	0
Cu-fcc	${}^0L^{Cu\text{-}fcc}$	−21923.39	5.37
Mg_2Cu	ΔG_f	−28620.00	0.03
$MgCu_2$ (Mg%, Cu)$_8$ (Cu%, Mg)$_{16}$	${}^0G^{MgCu_2}_{Cu:Cu}$	16743.20	0
	${}^0G^{MgCu_2}_{Mg:Cu}$	−37684.26	0
	${}^0G^{MgCu_2}_{Cu:Mg}$	0	0
	${}^0G^{MgCu_2}_{Mg:Mg}$	6278.7	0
	${}^0L^{MgCu_2}_{Mg,Cu:Cu}$	13011.35	0
	${}^0L^{MgCu_2}_{Mg,Cu:Mg}$	13011.35	0
	${}^0L^{MgCu_2}_{Cu:Mg,Cu}$	6599.45	0
	${}^0L^{MgCu_2}_{Mg:Mg,Cu}$	6599.45	0

experimental information from the literature. Various pieces of information related to the Gibbs free energy can be taken as input data for the optimization that includes crystallographic information. All relevant data should be critically evaluated to choose the most reliable sets to be used for the optimization [15].

3.1. The Mg–Cu binary system

3.1.1. Phase diagram

The Mg–Cu system was evaluated by Boudouard [16], Sahmen [17], and Urazov [18]. They reported the existence of two congruently melting compounds, and three eutectic points in the system. The analysis of Boudouard [16] showed one more line compound and one eutectic point which was, however, not accepted by other researchers [17–19]. The most extensive work on the Mg–Cu system was done by Jones [19] using both thermal and microscopic analyses. His reported data were not fully consistent with the previous authors. Since he used a huge number of samples and took extreme precautions during the sample preparations, his results are more reliable and will be used in this work.

No homogeneity range is mentioned for the intermediate phase of Mg_2Cu, whereas $MgCu_2$ was reported with a narrow homogeneity range that extends on both sides of the stoichiometric composition. Grime and Morris-Jones [20] showed a homogeneity range of (2 to 3) at.% on both sides of the stoichiometry. Also, X-ray diffraction from Sederman [21] disclosed that the extent of solubility on both sides of $MgCu_2$ at $T = 773$ K does not exceed 2.55 at.% (from 64.55 to 67.20) at.% Cu and considerably less at lower temperatures. However X-ray diffraction, microscopic, simple, and differential thermal analysis by Bagnoud and Feschotte [11] confirmed that the maximum solid solubility at the eutectic temperatures on both sides of $MgCu_2$ are (64.7 and 69) at.% Cu.

Hansen [22] reported that the solubility of Cu in Mg increases from about 0.1 at.% Cu at room temperature to about (0.4 to 0.5) at.% Cu at $T = 758$ K. However, Jenkin [23] was doubtful about the accuracy of the above solubility limit and reported that the limit should be very much less. The metallography of the high-purity alloys prepared by Jenkin [23] clearly indicated that the solubility of Cu in Mg is less than 0.02 at.% Cu at $T = 723$ K. Elaborate metallographic analysis of Jones [19] also showed that the solubility of Cu in Mg is only 0.007 at.% Cu at room temperature, increasing to about 0.012 at.% Cu near the eutectic temperature. These values are contradictory to those given by Hansen [22]. Later, Stepanov and Kornilov [24] revealed that the solubility is 0.2 at.% Cu at $T = 573$ K, 0.3 at.% Cu at $T = 673$ K, and 0.55 at.% Cu at $T = 753$ K. This is in considerable agreement with the metallographic work of Hansen [22]. However considering the accuracy of the analysis by Jones and Jenkin [19,23], it appears that the solubility limits given in [22,24] are quite high. Hence in this work, the results of Jones [19] are used.

The solubility of Mg in Cu was determined by Grime and Morris-Jones [20]. According to their X-ray powder diffraction results, the maximum solubility is approximately 7.5 at.% Mg. According to Jones [19], the solubility is about 5.3 at.% Mg at $T = 773$ K, increasing to about 6.3 at.% Mg at $T = 1003$ K. Stepanov [25], however, determined the maximum solid solubility of 10.4 at.% Mg using an electrical resistance method. Bagnoud and Feschotte [11] placed the maximum solubility at 6.94 at.% Mg. Except for the results by Stepanov [25], most of the data [19,20,11] are in close agreement with each other. In this work, the results of Jones [19] have been used during optimization for their consistency in representing the entire phase diagram.

Thermodynamic modelling on Mg–Cu system was done by Nayeb-Hashemi and Clark [26], Coughanowr *et al.* [27], and Zuo and Chang [28]. The homogeneity range of $MgCu_2$ phase was reproduced by both [27,28] using the Wagner–Schottky [13] type model while, sub-lattice model was used in this work.

3.1.2. Thermodynamic data

Garg *et al.* [29], Schmahl and Sieben [30], Juneja *et al.* [31], and Hino *et al.* [32] measured the vapour pressure of Mg over Mg–Cu liquid alloys using different techniques. The activity measured by these four different groups is more or less in good agreement with each other. Enthalpy of mixing for the Mg–Cu liquid was measured by Sommer *et al.* [33] and Batalin *et al.* [34] using the calorimetric method. King and Kleppa [35] determined the enthalpies of formation for $MgCu_2$ and Mg_2Cu by the calorimetric method. Similar values have been determined by Eremenko *et al.* [36] using EMF measurements. The vapour pressure measurements of Smith *et al.* [37] showed discrepancy with the other results. Due to

different measurement techniques, the reported values are mutually contradictory. Since vapour pressure measurements usually do not provide highly reliable results, the values in [35,36] are considered more acceptable and hence were given higher weighing factors during optimization.

3.2. The Cu–Y binary system

3.2.1. Phase diagram

Domagala *et al.* [38] studied the Cu–Y system by metallographic method, X-ray analysis, and critical temperature work to construct the phase diagram. They reported the composition and temperature of four eutectic points, one peritectic point, and four intermediate compounds CuY, Cu_2Y, Cu_4Y, and Cu_6Y. They also reported the maximum solid solubility of Cu in Y as well as Y in Cu to be less than 1 wt%. It is worth noting that Domagala *et al.* [38] missed the presence of the Cu_7Y_2 compound. Massalski *et al.* [39] published a phase diagram of the Cu–Y system based on the experimental data of Domagala *et al.* [38]. Buschow and Goot [12] investigated the system by metallography and X-ray diffraction and obtained evidence for the existence of two hexagonal Cu-rich phases. They defined the composition as Cu_5Y, having a hexagonal $CaCu_5$ type structure and Cu_7Y, having a hexagonal $TbCu_7$ type structure. Chakrabarti and Laughlin [40] proposed a phase diagram for this system using the experimental data of Domagala *et al.* [38]. The information they provided on this system was incomplete especially with regard to the entire *liquidus* region. Various transition temperatures were also not accurately determined. Guojun *et al.* [41] measured the heat contents and determined the melting point of the intermetallic compounds using drop calorimeter in a temperature range of (850 to1300) K. Domagala *et al.* [38] determined the melting point by visual analysis of the samples and reported error of measurement by ±15 K. This method is not precise and therefore the data reported by Guojun and Itagaki [41] are preferred. They determined the critical temperature of the intermetallic compounds by drop calorimetry by analyzing the deflection points in the J_T–T curve, where J_T is the heat content and T is the absolute temperature. Itagaki *et al.* [42] optimized the Cu–Y system using the experimental data of Guojun and Itagaki [41]. Unlike Chakrabarti and Laughlin [40], they considered Cu_4Y as a stoichiometric compound. However, all the experimental and calculated data reported by different authors are contradictory to one another. To resolve the controversy, Fries *et al.* [14] reinvestigated the Cu–Y system by DTA and XRD analysis, with emphasis on the range between (55 and 90) at.% Cu, and they proposed a new phase diagram. Their DTA results provide evidence for the possible existence of a high temperature phase transformation in the Cu_2Y compound {$Cu_2Y(h) \leftrightarrow Cu_2Y(r)$}. The invariant points obtained in [14] show fair agreement with the experimental data from Guojun *et al.* [41] but differ markedly from those of [38,39] along the (α-Y) *liquidus* line. Later, Abend *et al.* [43] made another attempt to investigate the Cu–Y system between (30 and 90) at.% Cu using EMF, DTA, and XRD. Their reported values are in fair agreement with those in [14,41] and differ from those in [38,39]. These results will be compared with the current assessment of the equilibria in the Cu–Y system.

The XRD results of Fries *et al.* [14] confirmed a range of solubility for the Cu_6Y phase. The limits of Y-rich and Cu-rich sides were determined to be (84.5 ± 0.5) at.% Cu and (87.0 ± 0.5) at.% Cu, respectively, over the temperature range of (973 to 1123) K. This is in reasonable agreement with the reported values (85.7 to 87.5) at.% Cu by Massalski *et al.* [39] and (84 to 88) at.% Cu by Okamoto [44]. Also, the emf measurement by Abend and Schaller [43] showed a similar range of homogeneity. The Cu_4Y phase is considered as a stoichiometric compound in this work since no definite homogeneity range was reported.

The experimental results available for the Cu–Y system are not in good accord with each other. However after reviewing all the available data for this system, it appears that the results of Guojun *et al.* [41] and Fries *et al.* [14] are the most reliable and therefore were given higher weighing factors during optimization.

3.2.2. Thermodynamic properties

The amount of thermodynamic data for the Cu–Y system is limited. The yttrium is highly reactive and hence it is very difficult to handle the alloys during high temperature experiments. However, heats of mixing of liquid Cu–Y alloys have been determined calorimetrically by Watanabe *et al.* [45] at T = 1373 K, Sudavtsova *et al.* [46] at T = 1415 K and also by Sidorov *et al.* [47] at T = 1963 K. Berezutskii and Lukashenko [48] measured the vapour pressure and activity coefficients of liquid Cu over the composition range of (19.8 to100) at.% Cu at T = 1623 K. Abend and Schaller [43] measured the activity of Y in the solid state using the emf measurement technique. Different thermodynamic properties of the Cu–Y liquid were calculated by Ganesan *et al.* [49]. Guojun *et al.* [41] and Watanabe *et al.* [45] determined the enthalpy of formation of CuY, Cu_2Y, and Cu_4Y. These values along with the reported values of Cu_6Y and Cu_7Y_2 by Itagaki *et al.* [42] will be compared with the current modelling results.

3.3. Mg–Y binary system

3.3.1. Phase diagram

Gibson *et al.* [50] were the first researchers who reported the Mg–Y phase diagram. They determined the maximum primary solid solubility of Y in Mg as 9 wt% Y at the eutectic temperature (840 K). This agrees well with the results of Sviderskaya and Padezhnova [51] who used thermal analysis to study the Mg-rich region of the Mg–Y system. Another investigation by Mizer and Clark [52] on this system using thermal analysis and metallography showed that the maximum solubility of Y in solid Mg was approximately 12.6 wt% Y at the eutectic temperature. This is, also, in good accord with the results of [50,51].

As reported by Gibson *et al.* [50], there is one eutectic reaction occurring at 74 wt% Mg and T = 840 K and one eutectoid reaction at 11 wt% Mg and T = 1048 K. The latter reaction was associated with a high temperature allotropic transformation of yttrium. Three intermediate phases were identified as γ at 21.5 wt% Mg, δ at 41 wt% Mg and ε at 60 wt% Mg. But any definite composition for these phases was not mentioned. However, ε and γ were reported to have compositions of $Mg_{24}Y_5$ and MgY, respectively, by Sviderskaya and Padezhnova [51].

The thermodynamic optimization of Ran *et al.* [53] showed a very good agreement with the measured values of Gibson *et al.* [50]. Massalski [54] assessed the Mg–Y phase diagram using the available experimental data from the literature. He used the experimental data of [51] for the Mg-rich region. Smith *et al.* [55] investigated the crystallography of MgY (γ), Mg_2Y (δ) and $Mg_{24}Y_5$ (ε) intermediate phases. The tangible homogeneity ranges of ε and γ determined by them will be compared with the current analysis. The δ-phase was predicted as a stoichiometric compound in [50,54,55]. Their results do not agree with Flandorfer *et al.* [56], who employed XRD, optical microscopy, and microprobe analyses to study the Ce–Mg–Y isothermal section at T = 773 K. Based on the experimental work of [56], the homogeneity range of δ-phase was obtained and will be compared with the current results. The X-ray diffraction analysis of Smith *et al.* [55] showed that γ-phase has CsCl type structure, δ-phase has $MgZn_2$structure, and ε-phase has α-Mn structure. Another investigation on the crystal structure of ε-phase by Zhang and Kelly [57] using transmission electron microscopy (TEM) showed the same structure as found by Smith *et al.* [55] but with one difference in the occupying atoms at the

2a Wyckoff position. However, since the work of Zhang and Kelly [57] used TEM, it is used during modelling of the ε-phase, because it is considered more precise than that of Smith *et al.* [55] where XRD was used. Thermodynamic investigations on the Mg–Y system were carried out by Fabrichnaya *et al.* [58] and Shakhshir and Medraj [59]. Both of them reproduced the homogeneity range of the intermetallic phases using the required crystallographic information but with two different approaches. However, for this work the same models reported by Shakhshir and Medraj [59] was used since their modelling approach was the same as the other intermetallic phases modelled in this work.

3.3.2. Thermodynamic data

Agrawal *et al.* [60] measured calorimetrically the enthalpy of mixing of the liquid Mg–Y alloy near the Mg-rich region (up to 21.8 at.% Y) at different temperatures. Activities of Mg was measured by Gansen *et al.* [49] using the vapour pressure technique which is in agreement with the results of Isper and Gansen [61] who used the same method for the measurement. The enthalpy of formation of all three compounds was determined calorimetrically by Pyagai *et al.* [62]. Their results are in reasonable agreement with the calorimetric data of Smith *et al.* [55] except for the γ-phase, for which the value of Pyagai *et al.* [62] is twice more negative than that obtained by Smith *et al.* [55]. This is due to the difficulties in measuring the enthalpy of formation when the yttrium content increases and hence the reactions become more exothermic. Also, Y has a high melting point compared to Mg and this leads to the sublimation of Mg during fusion of the metals [60]. The experimental results for enthalpy of formation of the compounds in the Mg–Y system will be compared with the current modelling results.

3.4. Mg–Cu–Y ternary system

Inoue *et al.* [3], Ma *et al.* [4], and Busch *et al.* [63] carried out some experimental investigations on the Mg–Cu–Y system to find the glass-forming ability at different compositions. However, their reported results cannot be used in this work since equilibrium conditions cannot be achieved during the preparation of amorphous material. Ganesan *et al.* [49] measured the enthalpy of mixing of the liquid by a calorimetric method along five different isopleths. Also, the activity of magnesium in the ternary liquid was reported by them. These results will be compared with the calculated values from the current work.

Two ternary compounds of composition Y_2Cu_2Mg and YCu_9Mg_2 were identified by Mishra *et al.* [64] and Solokha *et al.* [65]. However no thermodynamic properties for these compounds could be found in the literature. For this reason, it was not possible to include them in the present work by the conventional method. But for better understanding of the ternary system, these two compounds were included in the optimization by an alternative method which will be discussed later. A thermodynamic calculation of the Mg–Cu–Y system was carried out by Palumbo *et al.* [66]. They proposed a new modelling approach for the description of the specific heat of the liquid to include the glass transition phenomenon. The ternary compounds were not included in their assessment.

A complete thermodynamic optimization for the Mg–Cu–Y ternary system is still unknown. Also, the liquid phases of the three constituent binary systems Mg–Cu, Cu–Y, and Mg–Y need to be remodelled in order to consider the presence of short range ordering.

4. Results and discussion

4.1. The Mg–Cu binary system

4.1.1. Phase diagram

The calculated Mg–Cu phase diagram is shown in figure 1 which shows reasonable agreement with the experimental data from the literature. All the optimized parameters are listed in table 4. The excess entropy term (b) for the Mg_2Cu phase is 0.03 $J \cdot mol^{-1} \cdot K^{-1}$ which is very close to zero. Although it is desired to reduce the number of parameters, it is very difficult to get exact zero value for this term because for modelling the stoichiometric phase using the FactSage software [69], one needs to provide some entropy value for the compound and the change of entropy is calculated using the corresponding reaction. The congruent melting temperature of $MgCu_2$ was calculated as 1061 K. The experimental values of temperature reported in [17,18,11] are 1070 K, 1072 K, and (1066 ± 4) K, respectively. On the other hand, Jones [19] determined this

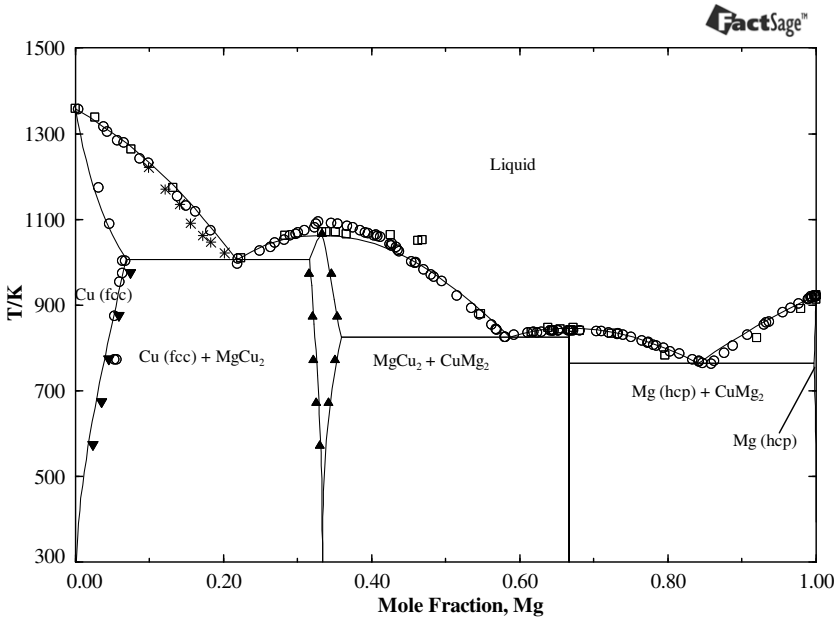

FIGURE 1. Plot of temperature against mole fraction Mg to illustrate the calculated Mg–Cu phase diagram: ▲: [11], □: [17], ∗: [18], ○: [19], ▼: [67].

melting temperature as 1092 K which is not consistent with the other experimental values. This may be because it is an old measurement (1931). Hence, it was decided to be consistent with the most recent value reported by Bagnoud and Feschotte [11]. Also, the homogeneity range of $MgCu_2$ is consistent with the experimental data of Bagnoud and Feschotte [11]. The remaining parts of the

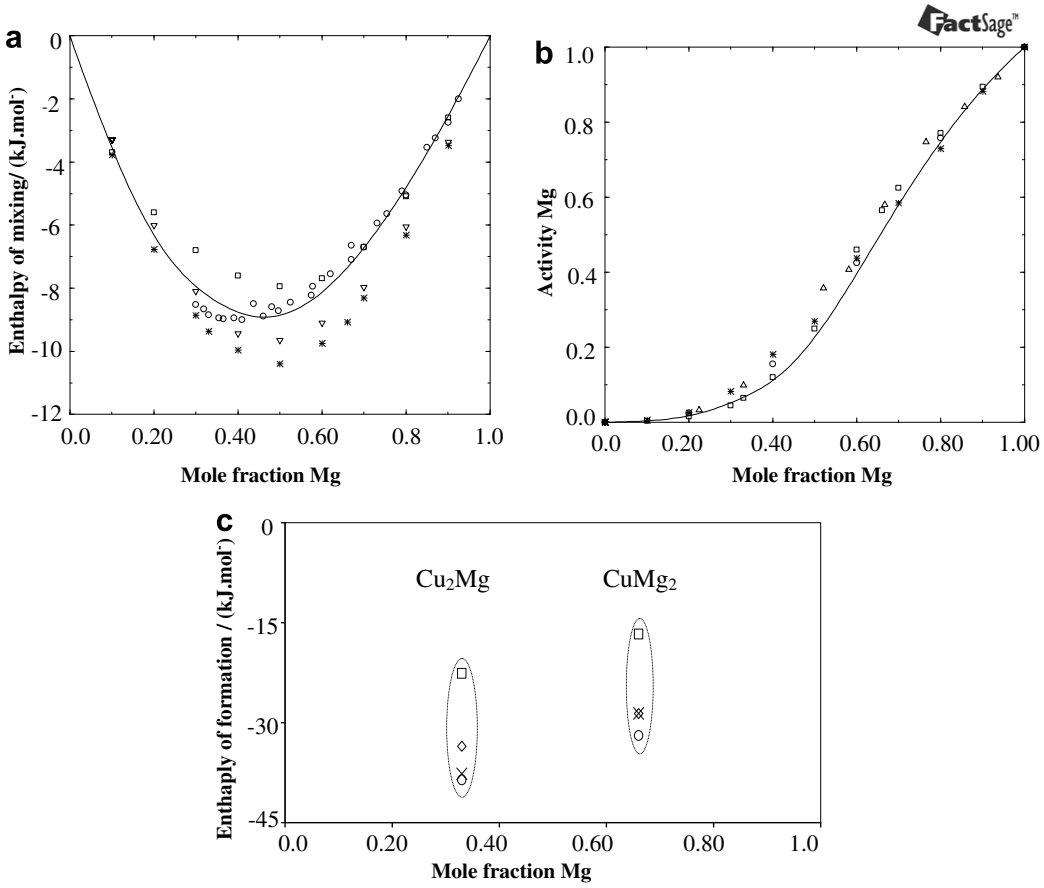

FIGURE 2. Plot of calculated thermodynamic properties against mole fraction Mg with the literature values: (a) enthalpy of mixing in $kJ \cdot mol^{-1}$ for the Mg–Cu liquid at $T = 1100$ K: ▽: [29] at 1100 K, ∗: [31] at 1100 K, ○: [33] at 1120 K and 1125 K, □: [34] at 1100 K. (b) Activity of Mg in the Mg–Cu liquid at $T = 1123$ K: ∗: [29] at 1100 K, △: [30] at 1123 K, □: [31] at 1100 K, ○: [32] at 1100 K. (c) Enthalpy of formation in $kJ \cdot mol^{-1}$ for the stoichiometric compounds: × : [this work], ◇: [35], ○: [36], □: [37].

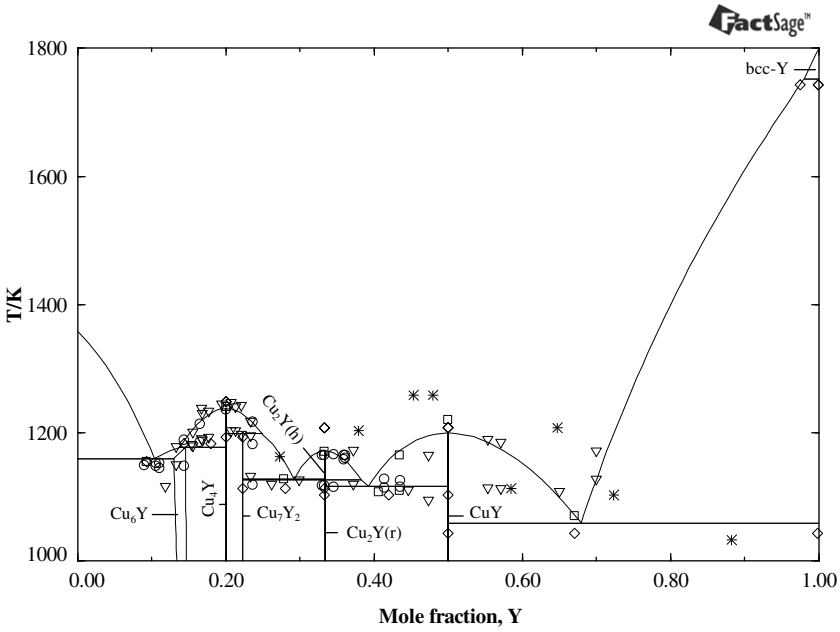

FIGURE 3. Plot of temperature against mole fraction Y to illustrate the calculated Cu–Y phase diagram: ○: [14], ∗ [38], ◇: [39], □: [41], ∇: [43].

phase diagram are in fair *agreement with the experimental data from the literature*.

4.1.2. Thermodynamic properties

The calculated enthalpy of mixing, shown in figure 2a, is in good agreement with the experimental data. The calculated activity of Mg in Mg–Cu liquid at $T = 1100$ K is shown in figure 2b which agrees well with the experimental results from the literature [29–32]. The experimental data for the activity of Cu could not be found in the literature. Figure 2c shows good agreement between the calculated heats of formation of $MgCu_2$ and Mg_2Cu, obtained in this study and the experimental results reported by King and Kleppa [35] and Eremenko *et al.* [36]. The measured values of Smith and Christian [37] are less negative than those calculated and also inconsistent with other experimental results. This is probably due to the inaccuracy involved in the vapour pressure measurement carried out by Smith and Christian [37].

TABLE 5
Optimized model parameters for the liquid, CuY, Cu_2Y(h), Cu_2Y(r), Cu_4Y, Cu_7Y_2, and Cu_6Y phases

Phase	Terms	a/(J · mol^{-1})	B/(J · mol^{-1} · K^{-1})
Liquid	Δg°_{AB}	−28718.77	6.28
	g^{lo}_{AB}	−6278.70	0.84
	g^{zj}_{AB}	−6906.57	2.09
Cu_6Y (Y%, Cu_2) $(Cu)_5$	$G^{Cu_6Y}_{Cu:Cu} - 7G^{hcp}_{Cu}$	0	0
	$G^{Cu_6Y}_{Cu:Y} - 5G^{hcp}_{Cu} - G^{hcp}_{Y}$	65.8	0
	${}^{0}L^{Cu_6Y}_{Y,Cu_2:Cu}$	− 4794.8	0.45
CuY	ΔG_f	−22517.5	−3.311
Cu_2Y (h)	ΔG_f	−17416.2	1.63
Cu_2Y (r)	ΔG_f	−21997.9	−2.44
Cu_4Y	ΔG_f	−17,888	−1.65
Cu_7Y_2	ΔG_f	−18775.5	−1.73

4.2. The Cu–Y binary system

4.2.1. Phase diagram

The Cu–Y calculated phase diagram with the available experimental data from the literature is shown in figure 3. The solid solubilities of Y in Cu and Cu in Y are negligible and hence were not included in this work. The optimized parameters are shown in table 5. Except few discrepancies with the results from Domagala [38], the phase diagram shows reasonable agreement with all the other experimental points. Composition of the eutectic point near the Cu-rich side shows small deviation from the experimental data. But the thermodynamic properties especially the enthalpy of mixing near the Cu-rich side shows strong agreement with the experimental data; hence this amount of error is acceptable. It is worth noting that trying to be consistent with the experimental eutectic composition resulted in deviation from the experimental thermodynamic properties of the Cu–Y liquid. The solid phase transformation of $Cu_2Y(h) \leftrightarrows Cu_2Y(r)$ was included in the current assessment

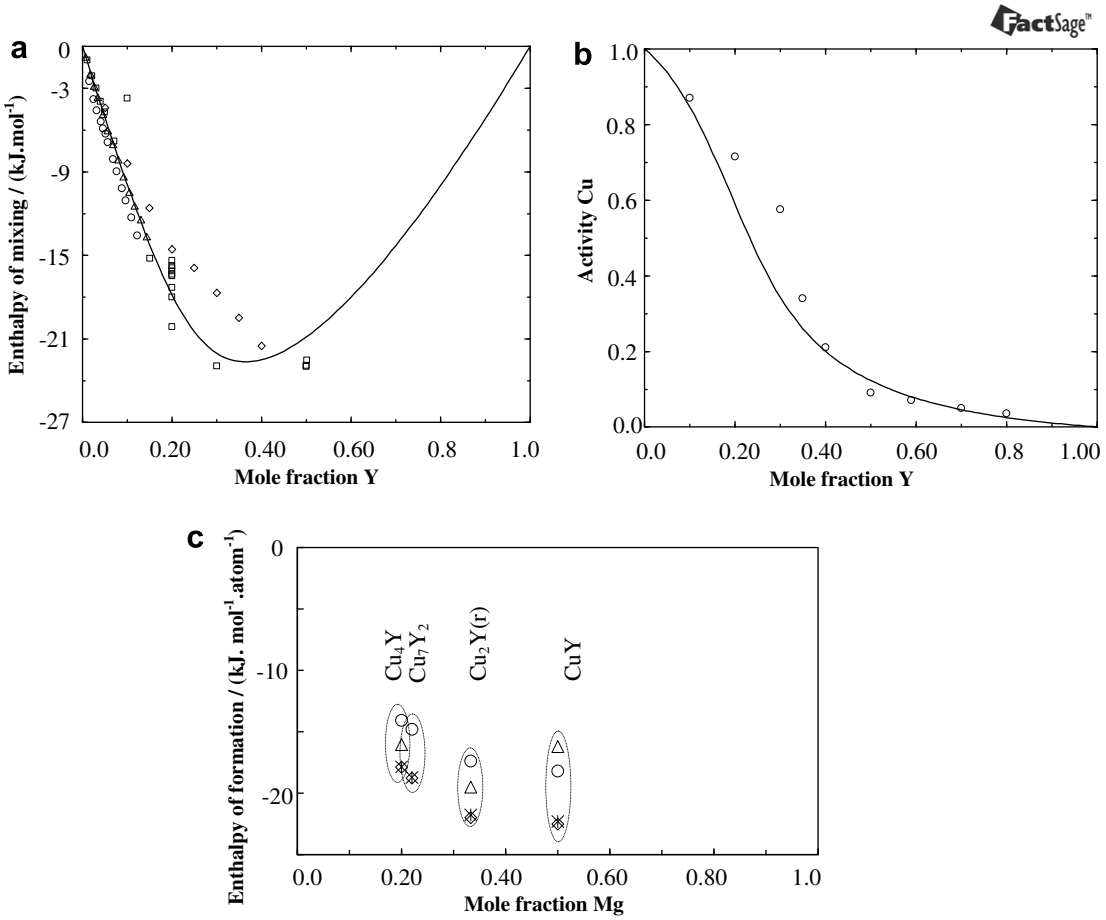

FIGURE 4. Plot of calculated thermodynamic properties against mole fraction with literature values: (a) enthalpy of mixing in kJ · mol^{-1} for the Cu–Y liquid at $T = 1410$ K: □: [45] at 1373 K, ○, ∇: [46] at 1410 K ◇: [47] at 1963 K. (b) Activity of Cu in the Cu–Y liquid at $T = 1623$ K; ○: [48] at 1623 K. (c) Enthalpy of formation in kJ · mol^{-1} for the stoichiometric compounds: ◇: [this work], : [14], △: [42], ○: [45].

of this system and the temperature and composition of the two eutectic points around this compound remained within the limits of the experimental errors.

4.2.2. Thermodynamic properties

The calculated enthalpy of mixing of the Cu–Y liquid at $T = 1410$ K in relation to the experimental results from the literature is shown in figure 4a. The calculated activity of Cu at $T = 1623$ K is shown in figure 4b, which is in good agreement with the experimental results of Berezutskii and Lukashenko [48] near the Y-rich corner. The curve shows some deviation from the experimental values between (20 and 35) at.% Y. However, the calculation of Ganesan *et al.* [49] showed very similar results to the present calculation. A comparison between the calculated enthalpy of formation for the stoichiometric compounds and other works is shown in figure 4c. Discrepancy can be seen between the different experimental works which is not unexpected since both Cu and Y are highly reactive elements and it is very difficult to perform any kind of experimental investigation on this system. Nevertheless, the results obtained in this work lie within the error limits of the experimental measurements.

4.3. The Mg–Y binary system

4.3.1. Phase diagram

The calculated phase diagram is shown in figure 5 with the experimental data from the literature. The optimized parameters are listed in table 6. The homogeneity ranges of the ε, δ, and γ phases were reproduced using the same models reported by Shakhshir and Medraj [59] with a fewer number of excess Gibbs free energy parameters. The models reported by Shakhshir and Medraj [59] are acceptable since both crystallographic information and homogeneity range data were taken into consideration during modelling process.

4.3.2. Thermodynamic properties

The calculated enthalpy of mixing at $T = 984$ K is shown in figure 6a with the available experimental data in the literature. The activity of Mg in liquid Mg–Y at $T = 1173$ K is shown in figure 6b which shows very good agreement with the experimental works in [49,61]. Better fit with the experimental data than the calculations of [58,59] was achieved in this work. The calculated partial Gibbs free energy of mixing of Mg and Y in the Mg–Y liquid at $T = 1173$ K shows good agreement with the experimental results of [63] as shown in figure 6c. Figure 6d shows the calculated

TABLE 6
Optimized model parameters for liquid, hcp-Mg, β-Y, ε, δ, and γ phases in Mg–Y system

Phase	Terms	A/(J · mol^{-1})	b/(J · mol^{-1} · K^{-1})
Liquid	Δg°_{MgY}	−13059.70	6.45
	g^{fo}_{MgY}	−13394.56	7.20
	g^{oj}_{MgY}	−6529.85	1.26
hcp-Mg	${}^0L^{Mg\text{-}hcp}$	−12476.78	7.49
	${}^1L^{Mg\text{-}hcp}$	−2724.56	2.4
	${}^2L^{Mg\text{-}hcp}$	−8788.22	2
β-Y	${}^0L^{Y\text{-}\beta}$	−29760.18	13.49
	${}^1L^{Y\text{-}\beta}$	−2005.86	1.5
ε (Mg%, Y)$_{29}$ (Y%, Mg)$_{10}$ (Mg)$_{19}$	${}^0G^{\varepsilon}_{Mg:Mg:Mg}$	1585	0
	${}^0G^{\varepsilon}_{Mg:Y:Mg}$	−5891.23	0
	${}^0G^{\varepsilon}_{Y:Y:Mg}$	6000	0
	${}^0G^{\varepsilon}_{Y:Mg:Mg}$	0	0
δ(Mg%, Y)$_6$ (Y%, Mg)$_4$ (Mg)$_2$	${}^0G^{\delta}_{Mg:Mg:Mg}$	2148.82	0
	${}^0G^{\delta}_{Mg:Y:Mg}$	−8902.47	0
	${}^0G^{\delta}_{Y:Y:Mg}$	0	0
	${}^0G^{\delta}_{Y:Mg:Mg}$	0	0
	${}^0L^{\delta}_{Mg,Y:Mg:Mg}$	9006.45	88.50
	${}^0L^{\delta}_{Mg,Y:Y:Mg}$	641.82	11.86
	${}^0L^{\delta}_{Mg:Mg,Y:Mg}$	−3910.07	3.46
	${}^0L^{\delta}_{Y:Mg,Y:Mg}$	9006.45	88.50
γ(Mg%, Y) (Y%: Va)	${}^0G^{\gamma}_{Mg:Y}$	−10727.25	1.26
	${}^0G^{\gamma}_{Mg:Va}$	10464.50	0.0
	${}^0G^{\gamma}_{Y:Y}$	13432.86	0
	${}^0G^{\gamma}_{Y:Va}$	13483.55	0
	${}^0L^{\gamma}_{Mg,Y:Y}$	15006.45	16
	${}^0L^{\gamma}_{Mg,Y:Va}$	15006.45	15
	${}^0L^{\gamma}_{Mg:Y,Va}$	−5000	7
	${}^0L^{\gamma}_{Y:Y,Va}$	−5000	7

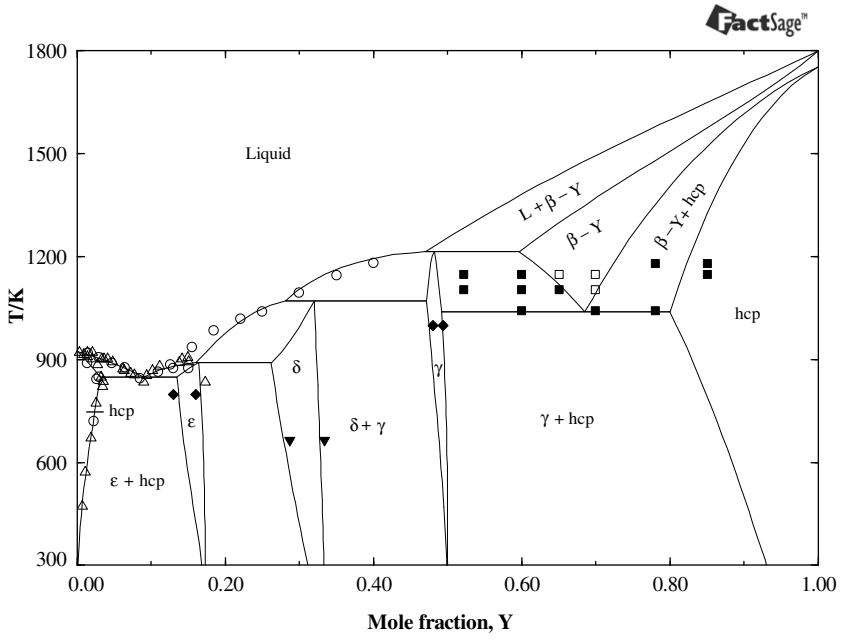

FIGURE 5. Plot of temperature against mole fraction yttrium to illustrate the calculated Mg–Y phase diagram: ○: [50], □: one phase region [50], ■: two phase region [50], △: [51], ♦: [55], ▼: [56].

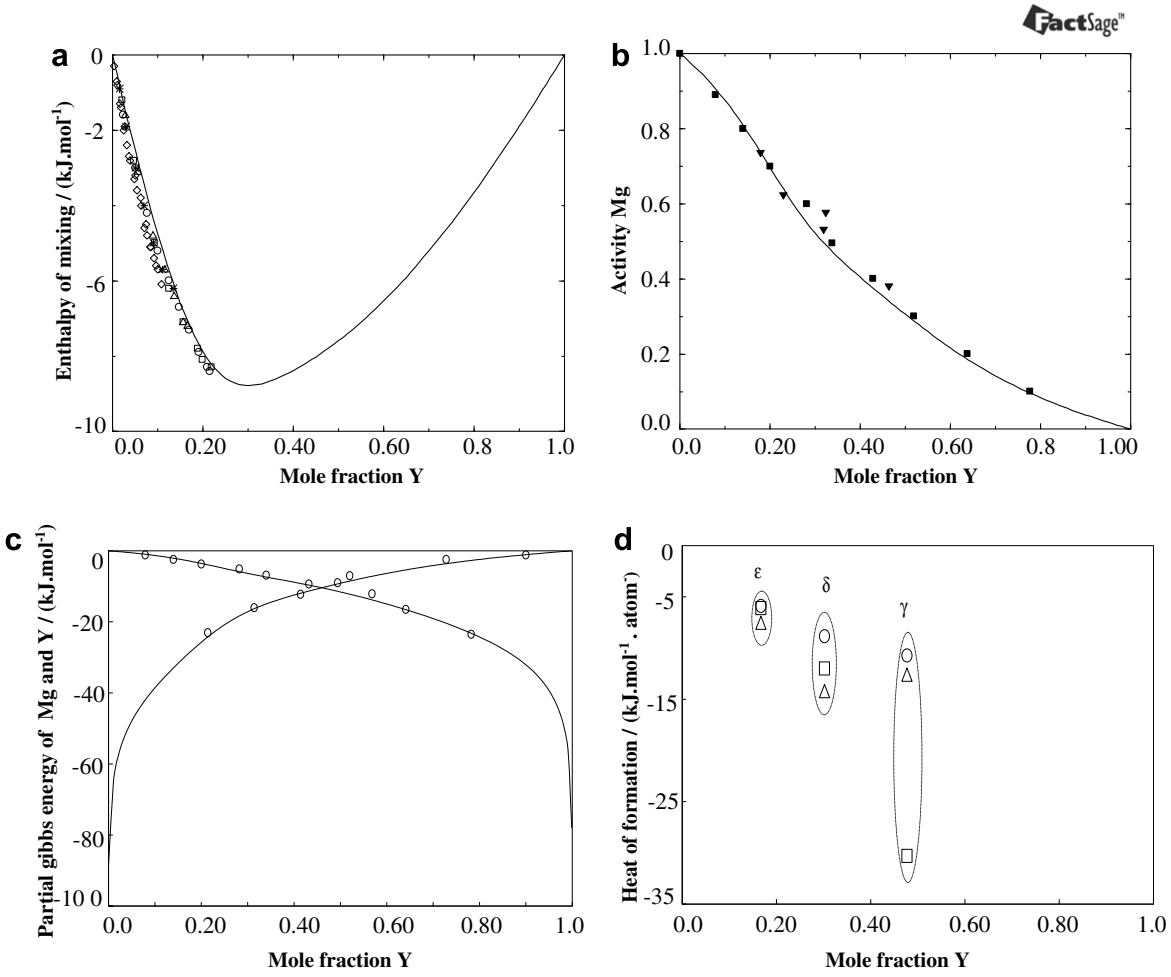

FIGURE 6. Plot of calculated thermodynamic properties against mole fraction yttrium with literature values: (a) enthalpy of mixing in kJ · mol^{-1} for the Mg–Y liquid at T = 984 K: □: at 1020 K, ○: at 1057 K, △: at 984 K, ◇: at 975 K, : at 955 K. [60]. (b) Activity of Mg in the Mg–Y liquid at T = 1173 K: ■: [49] at 1173 K, ▼: [61] at 1173 K. (c) Partial Gibbs free energy of mixing of Mg and Y at T = 1173 K: ○: [49]. (d) Enthalpy of formation in kJ · mol^{-1} for the stoichiometric compounds: ○: [this work], △: [55], □: [62].

enthalpy of formation of the intermediate compounds in the Mg–Y system in relation to the experimental results from the literature. A good agreement between the calculated and the experimental data of Smith *et al.* [55] and Pyagai *et al.* [62] can be seen. However, the enthalpy of formation for the γ phase measured by Pyagai *et al.* [62] is not consistent with the experimental value of Smith *et al.* [55] and the calculated value in this work. However, the results of Smith *et al.* [55] are more reliable since they used both the calorimetric and vapour pressure techniques in their investigation.

4.4. The Mg–Cu–Y system

A self-consistent thermodynamic database for the Mg–Cu–Y system has been constructed by combining the thermodynamic descriptions of the three constituent binaries Mg–Cu, Cu–Y, and Mg–Y. For the extrapolation of the ternary system, the Kohler geometric model [70] was used since none of the three binary systems showed much dissimilarity in their thermodynamic characteristics.

4.4.1. Phase diagram

The *liquidus* projection shown in figure 7 was calculated using FactSage software [69] with the optimized parameters of the three constituent binary systems without introducing any ternary interaction parameters.

The univariant valleys are shown by the heavier lines and the arrows on these lines indicate the directions of decreasing temperature. There are four ternary eutectic (E_1 to E_4) points, eight ternary quasi-peritectic (U_1 to U_8) points and three maximum (m_1 to m_3) points present in this system. A summary of the reactions at these invariant points is given in table 7.

4.4.2. Thermodynamic properties

Ganesan *et al.* [49] measured the enthalpy of mixing of the ternary Mg–Cu–Y liquid alloys by calorimetric method along five different isopleths. Their results were compared with the present calculated enthalpy of mixing for three different sections as shown in figures 8a to c. The initial discrepancy with the experimental results in figure 8c reflects the fact that the results of Ganesan *et al.* [49] for the enthalpy of mixing of ternary alloys is not consistent with the experimental binary enthalpy of mixing for the Cu–Y liquid.

The calculated activity of Mg in the ternary liquid alloy at T = 1173 K is shown in figure 8d, with the experimental data of Ganesan *et al.* [49]. The calculated values showed negative deviation from Raoult's law unlike the measured activity that showed positive deviation. The reason for this is not known. Nevertheless, the present calculated activity of Mg showed similar trend as the one calculated by Ganesan *et al.* [49] who, also, could not explain this inconsistency.

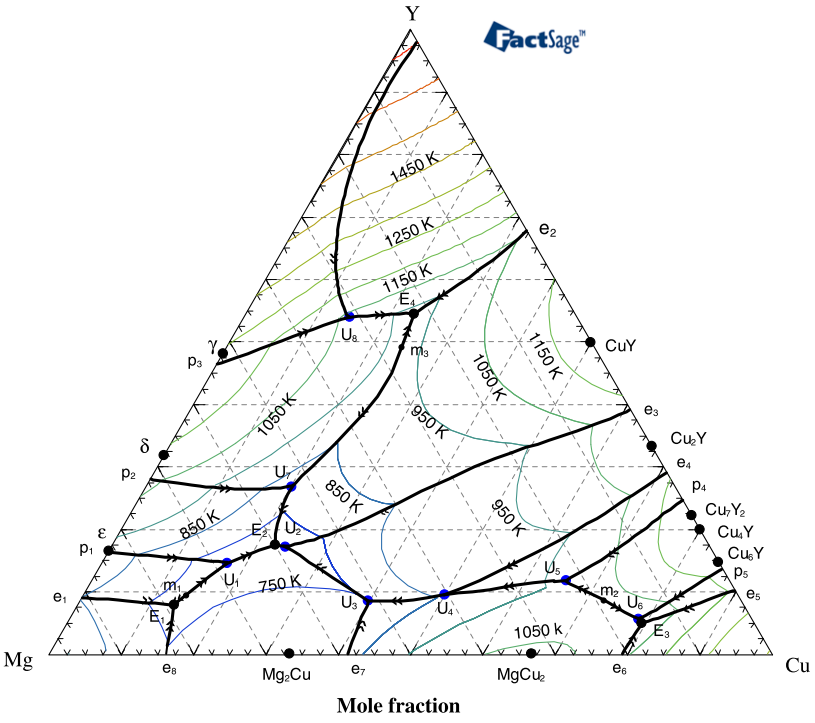

FIGURE 7. *Liquidus* projection of Mg–Cu–Y ternary system.

TABLE 7
Calculated equilibrium points and their reactions in the Mg–Cu–Y system

No.	Reaction	Calculated (this work)				
		T/K	Type	Y/at.%	Mg/at.%	Cu/at.%
1	Liquid ⇆ hcp-Mg + ε + $CuMg_2$	709.8	E_1	7.7	79.2	13.1
2	Liquid ⇆ δ + $CuMg_2$ + CuY	662.6	E_2	17.8	59.6	22.6
3	Liquid ⇆ Cu_6Y + $MgCu_2$ + Cu	956.3	E_3	5.1	15.9	79
4	Liquid ⇆ γ + hcp-Y + CuY	910.1	E_4	54.6	22.4	23
5	Liquid + ε ⇆ δ + Mg_2Cu	680.9	U_1	14.7	67.9	17.3
6	Liquid + Cu_2Y ⇆ CuY + $CuMg_2$	672.89	U_2	17.4	58.3	24.3
7	Liquid + $MgCu_2$ ⇆ $CuMg_2$ + Cu_2Y	761.22	U_3	8.8	51.4	39.8
8	Liquid + Cu_7Y_2 ⇆ $MgCu_2$ + Cu_2Y	849.4	U_4	9.8	40.6	49.6
9	Liquid + Cu_4Y ⇆ $MgCu_2$ + Cu_7Y_2	957.4	U_5	10.6	25.2	64.2
10	Liquid + Cu_4Y ⇆ Cu_6Y + $MgCu_2$	961.4	U_6	5.8	15.9	78.3
11	Liquid + γ ⇆ δ + CuY	794.23	U_7	27.3	52.2	20.5
12	Liquid + β-Y ⇆ hcp-Y + γ	1038	U_8	54	32.1	13.9
13	Liquid ⇆ ε + Mg_2Cu	710.5	m_1	8.8	77.4	13.8
14	Liquid ⇆ $MgCu_2$ + Cu_4Y	995.5	m_2	8.0	19.9	72.1
15	Liquid ⇆ γ + CuY	918.3	m_3	49.6	26.1	24.3

4.5. Approximation of the Mg–Cu–Y system with ternary intermetallics

Two ternary compounds Y_2Cu_2Mg and YCu_9Mg_2 were reported in the literature by Mishra *et al.* [64] and Solokha *et al.* [65], but information on melting temperatures or the enthalpies of formation of these compounds could not be found in the literature. The only available information is the annealing temperatures of these two compounds. Annealing was used by Mishra *et al.* [64] and Solokha *et al.* [65] to grow single-crystals in the samples. The reported annealing temperatures of Y_2Cu_2Mg and YCu_9Mg_2 are 900 K and 673 K, respectively. This means that these ternary compounds are stable at the annealing temperatures, and most probably they exist at low temperatures.

In order to reflect this important information in our work, we have created the approximate thermodynamic model of the Mg–Cu–Y system with ternary intermetallics. Absence of experimental data on melting temperatures and the enthalpies of formation of these compounds limited our thermodynamic model, but it could be useful for the readers who are interested in the ternary phase equilibrium below $T = 600$ K.

The *liquidus* surface in this model may have substantial deviations from reality because only indirect experimental data were available to approximate the melting temperatures of ternary compounds. That forced us to make some assumptions based on the available experiments on amorphous Mg–Cu–Y alloys and binary phase diagrams.

Inoue *et al.* [3] and Ma *et al.* [4] studied the Mg–Cu–Y system to find suitable compositions for metallic glass. They used XRD and DSC analyses to examine different amorphous samples. During their experiments, proper equilibrium conditions did not prevail, hence their experimental results cannot be used directly in this work. But after reviewing their [3,4] works, some information regarding the system can be obtained. The DSC analysis of Ma

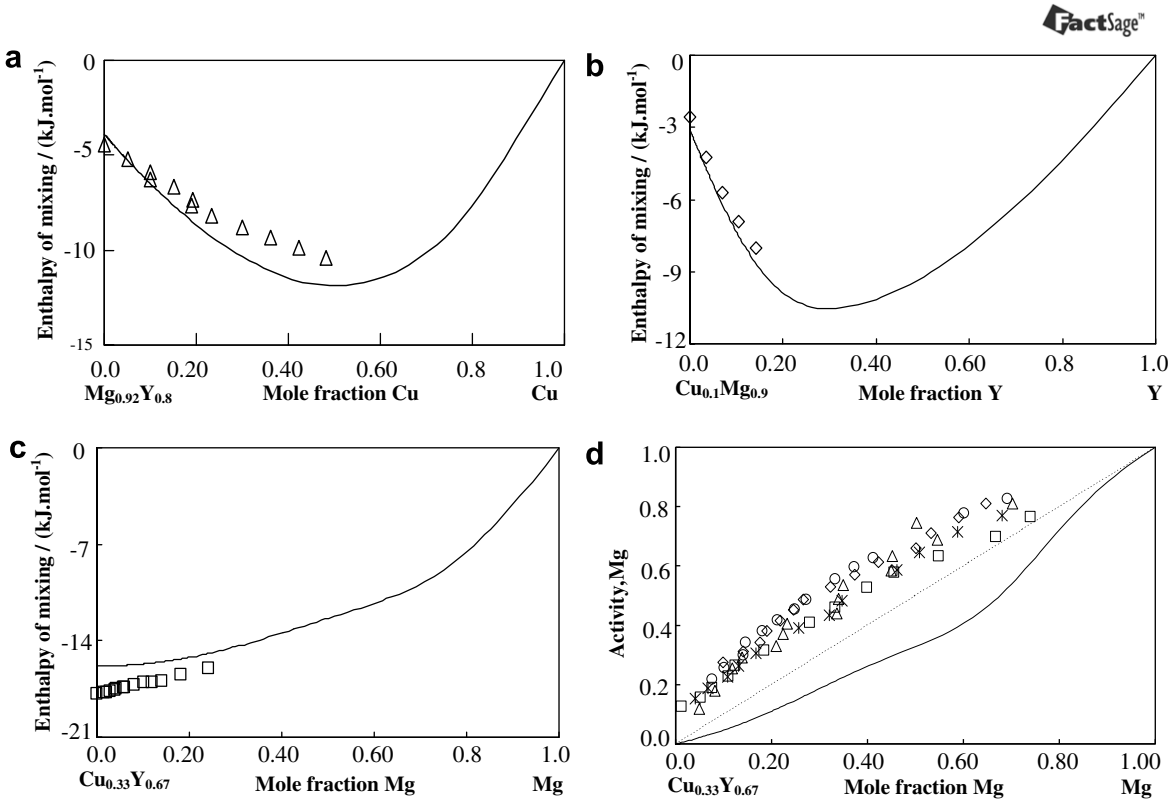

FIGURE 8. Plot of thermodynamic properties against mole fraction for the Mg–Cu–Y liquid: integral enthalpy of mixing in kJ · mol^{-1} for (a) $(Mg_{0.92}Y_{0.08})_{1-x}Cu_x$ ternary liquid at $T = 1023$ K: △: [49] at 1023 K. (b) $(Cu_{0.1}Mg_{0.9})_{1-x}Y_x$ ternary liquid at $T = 1023$ K: ◇: [49] at 1023 K. (c)$(Cu_{0.33}Y_{0.67})_{1-x}Mg_x$ ternary liquid at $T = 1107$ K: □: [49] at 1107 K. (d) Activity of Mg at $T = 1173$ K, --- ideal mixing: △, □, ◇, ○: [49].

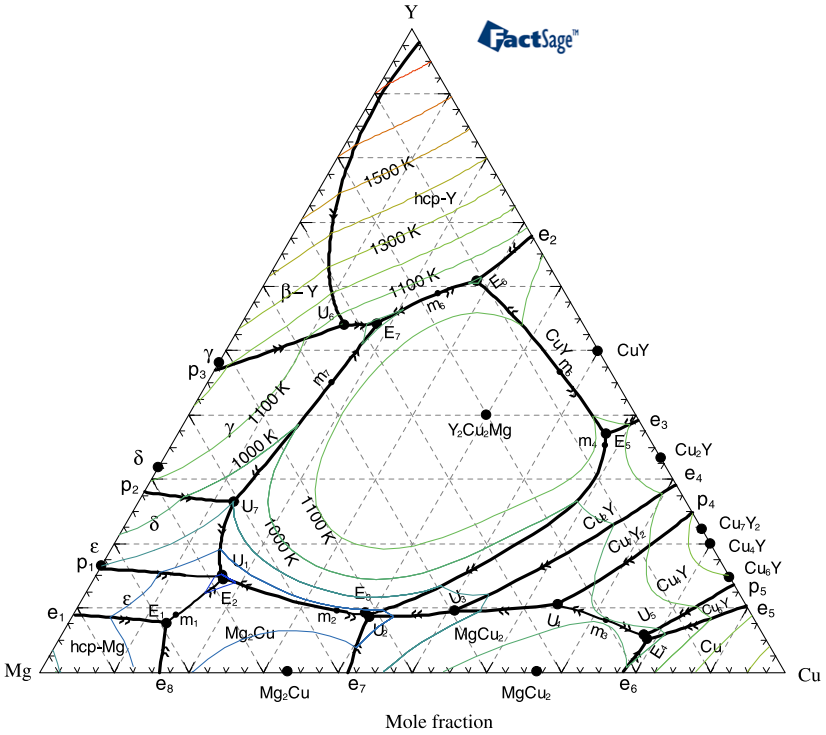

FIGURE 9. *Liquidus* projection of the Mg–Cu–Y system with the ternary compounds (tentative).

TABLE 8
Calculated equilibrium points and their reactions in the Mg–Cu–Y system after including the ternary compounds (tentative)

No.	Reaction	Calculated (this work)				
		T/K	Type	Y/at.%	Mg/at.%	Cu/at.%
1	Liquid ⇆ hcp-Mg + ε + $CuMg_2$	709.8	E_1	7.7	79.2	13.1
2	Liquid ⇆ δ + $CuMg_2$ + Y_2Cu_2Mg	682.0	E_2	14.6	68.1	17.3
3	Liquid ⇆ $CuMg_2$ + Cu_2Y + Y_2Cu_2Mg	760.8	E_3	9.0	51.6	39.4
4	Liquid ⇆ Cu_6Y + $MgCu_2$ + Cu	956.3	E_4	5.1	15.9	79.0
5	Liquid ⇆ Cu_2Y + CuY + Y_2Cu_2Mg	1059.9	E_5	37.1	5.5	57.4
6	Liquid ⇆ hcp-Y + CuY + Y_2Cu_2Mg	993.5	E_6	60.8	11.1	28.1
7	Liquid + δ ⇆ ε + $CuMg_2$	684.1	U_1	14.8	68.1	17.1
8	Liquid + Cu_2Mg ⇆ Cu_2Y + $CuMg_2$	761.2	U_2	8.8	51.7	39.5
9	Liquid + Cu_7Y_2 ⇆ $MgCu_2$ + Cu_2Y	868.0	U_3	9.7	39.3	51.0
10	Liquid + Cu_4Y ⇆ $MgCu_2$ + Cu_7Y_2	957.2	U_4	10.6	25.4	64.1
11	Liquid + Cu_4Y ⇆ Cu_6Y + $MgCu_2$	961.4	U_5	6.0	15.7	78.3
12	Liquid + β-Y ⇆ hcp-Y + γ	1038	U_6	54.8	32.1	13.1
13	Liquid + γ ⇆ δ + Y_2Cu_2Mg	900.2	U_7	26.6	60.7	12.7
14	Liquid ⇆ ε + $CuMg_2$	710.54	m_1	8.7	77.5	13.8
15	Liquid ⇆ $CuMg_2$ + Y_2Cu_2Mg	766.1	m_2	9.6	55.5	34.9
16	Liquid ⇆ $MgCu_2$ + Cu_4Y	995.5	m_3	8.0	19.9	72.1
17	Liquid ⇆ Cu_2Y + Y_2Cu_2Mg	1062.4	m_4	35.5	6.4	58.1
18	Liquid ⇆ CuY + Y_2Cu_2Mg	1136.3	m_5	46.6	6.8	46.6
19	Liquid ⇆ hcp-Y + Y_2Cu_2Mg	1010.3	m_6	58.9	17.1	24.0
20	Liquid ⇆ γ + Y_2Cu_2Mg	1013.4	m_7	45.1	38.2	16.7

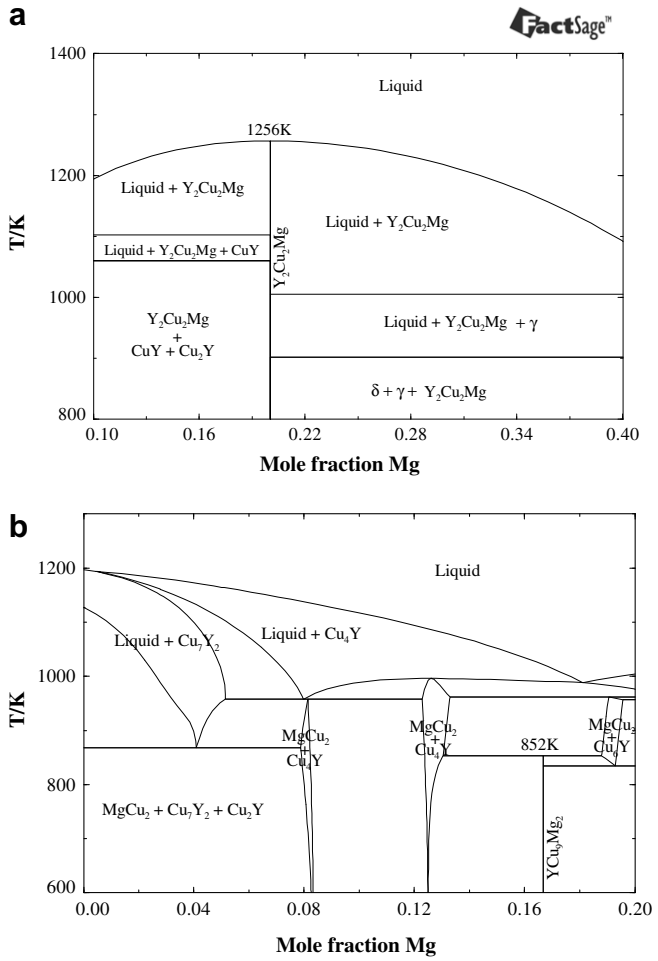

FIGURE 10. Plot of temperature against mole fraction Mg to show isopleths (constant composition section) of the Mg–Cu–Y system at (a) 40 at.% Y and at (b)-75 at.% Cu, showing the tentative melting temperature of Y_2Cu_2Mg and YCu_9Mg_2 compound, respectively (tentative).

et al. [4] shows that near $Mg_{65}Cu_{25}Y_{11}$ composition, a ternary eutectic point exists at a temperature around 730 K. Same composition for the eutectic was reported earlier by Inoue *et al.* [3]. Consequently, it can be assumed that the actual eutectic point would be found near this composition at a similar temperature, if proper equilibrium conditions are maintained. Depending on this information, the heat and entropy of formation of the ternary compounds were varied until the eutectic composition and temperature are close to those reported by Inoue *et al.* [3] and the melting temperatures for the ternary compounds were estimated from the resulting *liquidus* surface.

Based on the abovementioned assumptions, the *liquidus* projection was recalculated as shown in figure 9. The eutectic point (E_2) is observed at a composition of $Mg_{68}Cu_{17.3}Y_{14.6}$ and T = 682 K. The composition deviates from that of Inoue *et al.* [3] and Ma *et al.* [4] by about 8 at.% Cu and temperature around T = 50 K. A more accurate result can be obtained by introducing some ternary interaction parameters, but since the experimental data were not for equilibrium conditions, it was decided to accept the current calculation without using any interaction parameter. All the invariant points calculated after incorporating the ternary compounds are listed in table 8.

The melting temperature of the Y_2Cu_2Mg compound was adjusted to be 1256 K by a trial and error method, so that the eutectic composition and temperature lies in the desired range. The compound melts congruently at this temperature as can be seen in figure 10a.

The melting temperature of YCu_9Mg_2 should be lower than that of Y_2Cu_2Mg, since the overall Y content is less (8 *versus* 40 at.% Y). The reported annealing temperature (673 K), which is lower than that of Y_2Cu_2Mg, also supports this assumption. The XRD analysis of Ma *et al.* [4] on the alloy composition $Mg_{58.5}Cu_{30.5}Y_{11}$, shows the existence of Mg_2Cu, $Mg_{24}Y_5$ and one unidentified phase. It may be assumed that this unidentified phase is in fact the Y_2Cu_2Mg compound. To be consistent with this information, the melting temperature of YCu_9Mg_2 was adjusted to be 852 K. A vertical section for 75 at.% Cu in figure 10b shows that this compound melts incongruently. The presence of incongruently melting binary (Cu_6Y) compound near YCu_9Mg_2 also justifies this.

The above discussion shows the legitimacy of the current work. The analysis may not be totally accurate but at least it will give closer approximation of the actual equilibrium in the Mg–Cu–Y system. Some key experiments on this system may resolve this uncertainty. This should be attempted during further studies on this system.

5. Concluding remarks

A comprehensive thermodynamic assessment of the ternary Mg–Cu–Y system was conducted using available experimental data. Based on the current assessment, the following conclusions can be drawn:

- The modified quasichemical model was used to describe the liquid phase in the Mg–Cu–Y system. The calculated phase diagrams of the binary systems as well as thermodynamic properties such as activity, enthalpy of mixing, and enthalpy of formation of the compounds show good agreement with the experimental data available in the literature.
- A self-consistent database for the Mg–Cu–Y system was constructed by combining the optimized parameters of the three constituent binary systems. No ternary interaction parameters were used for the extrapolation.
- The presence of two ternary compounds was included in the optimization considering the limited experimental information available in the literature for these compounds.
- More experimental investigation is required to obtain detailed information regarding the two ternary compounds (Y_2Cu_2Mg and YCu_9Mg_2). The melting temperatures of these two compounds should be determined experimentally which is very important to establish a more accurate assessment of the Mg–Cu–Y system. Also, all the predicted invariant points in the Mg–Cu–Y ternary system are to be verified experimentally. The present work can be used to design key experiments for further verification of this system.

References

[1] J.M. Kim, K. Shin, K.T. Kim, W.J. Jung, Scripta Mater. 49 (2003) 687–691.
[2] R.H. Tendler, M.R. Soriano, M.E. Pepe, J.A. Kovacs, E.E. Vicente, J.A. Alonso, Intermetallics 14 (2006) 297–307.
[3] A. Inoue, A. Kato, T. Zhang, S.G. Kim, T. Masumoto, Mater. Trans. 32 (1991) 609–616.
[4] H. Ma, Q. Zheng, J. Xu, Y. Li, E. Ma, J. Mater. Res. 20 (2005) 2225–2252.
[5] H. Men, W.T. Kim, D.H. Kim, J. Non-Cryst. Solids 337 (2004) 29–35.
[6] A.T. Dinsdale, CALPHAD 15 (1991) 317–425.
[7] O. Redlich, A.T. Kister, J. Ind. Eng. Chem. 40 (1948) 341–345.
[8] A.D. Pelton, S.A. Degterov, G. Eriksson, C. Robelin, Y. Dessureault, Metall. Mater. Trans. B 31 (2000) 651–659.
[9] P. Chartrand, A.D. Pelton, Metall. Mater. Trans. A 32 (2001) 1397–1407.
[10] A.D. Pelton, P. Chartrand, G. Eriksson, Metall. Mater. Trans. A 32 (2001) 1409–1416.
[11] P. Bagnoud, P. Feschotte, Z. Metallkd. 69 (1978) 114–120.
[12] K.H.J. Buschow, A.S. Goot, Acta Crystallogr. B 27 (1971) 1085–1088.
[13] C. Wagner, W. Schottky, J. Phys. Chem. B 11 (1930) 163–210.
[14] S.G. Fries, H.L. Lukas, R. Konetzki, R. Schmid-Fetzer, J. Phase Equilibr. 15 (1994) 606–614.
[15] K.C. Kumar, P. Wollants, J. Alloys Compd. 320 (2001) 189–198.
[16] O. Boudouard, Comptes Rendus 135 (1902) 794–796.
[17] R. Sahmen, Z. Anorg. Allg. Chem. 57 (1908) 1–33.
[18] G.G. Urazov, Zh. Russ. Fiz. – Khim. Obschestva 39 (1907) 1556–1581.
[19] W.R.D. Jones, J. Jpn. Inst. Met. 574 (1931) 395–419.
[20] G. Grime, W. Morris-Jones, Philos. Mag. 7 (1929) 1113–1134.
[21] V.G. Sederman, Philos. Mag. 18 (1934) 343–352.
[22] M. Hansen, J. Jpn. Inst. Met. 428 (1927) 93–100.
[23] J.W. Jenkin, J. Jpn. Inst. Met. 428 (1927) 100–102.
[24] N.I. Stepanov, I.I. Kornilov, Izv. Inst. Fiz. – Khim. Analiza, Akad. Nauk SSSR 7 (1935) 89–98.
[25] N.I. Stepanov, Z. Anorg. Allg. Chem. 78 (1913) 1–32.
[26] A.A. Nayeb-Hashemi, J.B. Clark, Bull. Alloy Phase Diagram 5 (1984) 36–43.
[27] C.A. Coughanowr, I. Ansara, R. Luoma, M. Hämäläinen, H.L. Lukas, Z. Metallkd. 82 (1991) 574–581.
[28] Y. Zuo, Y.A. Chang, Z. Metallkd. 84 (1993) 662–667.
[29] S.P. Garg, Y.J. Bhatt, C.V. Sundaram, Metall. Mater. Trans. 4 (1973) 283–289.
[30] N.G. Schmahl, P. Sieben, in: NPL Symposium on Phys. Chem. of Metallic Solutions and Intermetallic Compounds, vol. 1, Paper 2K, 1960, pp. 268–282.
[31] J.M. Juneja, G.N.K. Iyengar, K.P. Abraham, J. Chem. Thermodyn. 18 (1986) 1025–1035.
[32] M. Hino, T. Nagasaka, R. Takehama, Metall. Mater. Trans. B 31 (2000) 927–934.
[33] F. Sommer, J.J. Lee, B. Predel, Ber. Bunsen-Ges. 87 (1983) 792–797.
[34] G.I. Batlin, V.S. Sudavtsova, M.V. Mikhailovskaya, Izv. Vysh. Ucheb. Zaved, Tsvetn Metall. 2 (1987) 29–31.
[35] R.C. King, O.J. Kleppa, Acta Mater. 12 (1964) 87–97.
[36] V.N. Eremenko, G.M. Lukashenko, R.I. Polotskaya, Izv. Akad. Nauk SSSR, Metall. 1 (1968) 210–212.
[37] J.F. Smith, J.L. Christian, Acta Mater. 8 (1960) 249–255.
[38] R.F. Domagala, J.J. Rausch, D.W. Levinson, Trans. Am. Soc. Met. 53 (1961) 137–155.
[39] T.B. Massalski, J.L. Murray, L.H. Bennett, H. Barker (Eds.), Binary Alloy Phase Diagrams, vol.1, ASM International, Materials Park, OH, 1986, pp. 977–978.
[40] D.J. Chakrabarti, D.E. E Laughlin, ASM Int. (1981) 478–481.
[41] Q. Guojun, K. Itagaki, A. Yazawa, Mater. Trans. 30 (1989) 273–282.
[42] K. Itagaki, Q.I. Guojun, A. Sabine, P.J. Spencer, CALPHAD 14 (1990) 377–384.
[43] U. Abend, H.J. Schaller, J. Phys. Chem. 101 (1997) 741–748.
[44] H. Okamoto, J. Phase Equilibr. 19 (1998) 398–399.
[45] S. Watanabe, O.J. Kleppa, Metall. Trans. B 15 (1984) 573–580.
[46] V.S. Sudavtsova, G.I. Vatalin, A.V. Kalmykov, F.F. Kuznetsov, Izv. Vysh. Ucheb. Zaved. Cvetn. Metall. 6 (1983) 107–108.
[47] O.Y. Sidorov, M.G. Valishev, Y.O. Esin, P.V. Gel'd, V.M. Zamyatin, A.Y. Dubrovski, Izv. Akad. Nauk SSSR, Metall. 4 (1990) 188–190.
[48] V.V. Berezutskii, G.M. Lukashenko, Zh. Fiz. Khim. 61 (1987) 1422–1424.
[49] V. Ganesan, F. Schuller, H. Feufel, F. Sommer, H. Ipser, Z. Metallkd. 88 (1997) 701–710.
[50] E.D. Gibson, O.N. Carlson, Trans. Am. Soc. Met. 52 (1960) 1084–1096.
[51] Z.A. Sviderskaya, E.M. Padezhnova, Izv. Akad. Nauk SSSR, Metall. 6 (1968) 183–190.
[52] D. Mizer, J.B. Clark, Trans. Am. Inst. Min. Met. Eng. 221 (1961) 207–208.
[53] Q. Ran, H.L. Lukas, G. Effenberg, G. Petzow, CALPHAD 12 (1988) 375–381.
[54] T.B. Massalski, H. Okamoto, P.R. Subramanian, L. Kacprzak (Eds.), Binary Alloy Phase Diagrams, second ed., vol. 3, ASM International, Materials Park, OH, 1990, pp. 2566–2569.
[55] J.F. Smith, D.M. Bailey, D.B. Novotny, J.E. Davison, Acta Mater. 13 (1965) 889–895.
[56] H. Flandorfer, M. Giovannini, A. Saccone, P. Rogl, R. Ferro, Metall. Mater. Trans. A 28 (1997) 265–276.
[57] M.X. Zhang, P.M. Kelly, Acta Mater. 53 (2005) 1085–1096.
[58] O.B. Fabrichnaya, H.L. Lukas, G. Effenberg, F. Aldinger, Intermetallics 11 (2003) 1183–1188.
[59] S. Shakhshir, M. Medraj, J. Phase Equilibr. Diffus. 27 (2006) 231–244.
[60] R. Agarwal, H. Feufel, F. Sommer, J. Alloys Compd. 217 (1995) 59–64.
[61] V. Ganesan, H. Ipser, J. Chim. Phys. 94 (1997) 986–991.
[62] I.N. Pyagai, A.V. Vakhobov, N.G. Shmidt, O.V. Zhikhareva, M.I. Numanov, Dokl. Akad. Nauk Tadzh. SSR 32 (1989) 605–607.
[63] R. Busch, W. Liu, L. Johnson, J. Appl. Phys. 83 (1998) 4134–4141.
[64] R. Mishra, R.D. Hoffmann, R. Pottgen, Z. Naturforsch. B 56 (2001) 239–244.
[65] P. Solokha, V. Pavlyuk, A. Saccone, S.D. Negri, W. Prochwicz, B. Marciniak, E.R. Sokolowska, J. Solid State Chem. 179 (2006) 3073–3081.
[66] M. Palumbo, M. Satta, G. Cacciamani, M. Baricco, Mater. Trans. 47 (2006) 2950–2955.
[67] I.L. Rogel'berg, Tr. Gos. Nauch. -Issled. Proekt. Inst. Obrab. Tsvet. Met. 16 (1957) 82–89.
[68] W.G. Wyckoff, Crystal Structures, second ed., vol. 1, John Wiley & Sons, New York, 1963. pp. 365-367.
[69] FactSage 5.4.1, Thermofact (Centre for Research in Computational Thermochemistry), Montreal, QC, Canada, 2006.
[70] F. Kohler, Monatsh. Chem. 91 (1960) 738–740.

JCT 07-365